

# Physical features of blends based in a liquid crystalline polymer: the effect of the mixing devices

Ane Zaldúa, M. Eugenia Muñoz, Juan J. Peña\* and Anton Santamaria

Departamento de Ciencia y Tecnología de Polímeros and \*Departamento de Física de Materiales, Facultad de Química/Kimika Fakultatea, Universidad del País Vasco/Euskal Herriko Unibertsitatea, Apartado 1072, 20080 San Sebastián, Basque Country, Spain  
(Received 5 August 1991)

Rheology, viscoelastic measurements and morphological aspects of blends of a commercial liquid crystalline polymer (LCP) and a polyarylate of bisphenol A (PAr) are presented. Viscoelastic results reveal incompatibility between the components and in the case of 60 LCP/40 PAr blends the physical properties are different, depending on the mixing method. This is attributed to the relationship between rheology, morphology and properties. The influence of the composition and the draw ratio on the storage tensile modulus is also studied.

(Keywords: thermotropic copolyesteramide; static mixer; dynamic viscoelasticity; draw ratio; rheology; morphology)

## INTRODUCTION

Since the first patents of liquid crystalline thermotropic copolyesters in the early 1970s, the number of industrial and academic studies on thermotropic polymers has been increasing. Today the variety of anisotropic polymers known is immense and technological applications involve copolyesters containing polymers obtained from symmetric monomers such as *p*-hydroxybenzoic acid, naphthoic acid, terephthalic acid and hydroquinone. The review by Calundann and Jaffe<sup>1</sup> summarizes the molecular architecture used to promote melt anisotropy at reasonable temperatures. These materials show good processibility and mechanical properties, but are expensive. In an attempt to use these polymers as reinforcing and processing aid agents of more classical thermoplastics, several studies have been undertaken in the last decade. Dutta *et al.*<sup>2</sup> and Brostow<sup>3</sup> have reviewed the literature for this type of blends and the topic that has been most widely investigated is the development of a fibrillar morphology of the dispersed liquid crystalline polymer.

In this paper we present rheological and viscoelastic measurements, as well as morphological aspects, of the blends of a commercial liquid crystalline copolyesteramide and a polyarylate of bisphenol A (PAr). The thermotropic copolyesteramide used is Vectra<sup>®</sup> B950 (Hoechst-Celanese), which has not received as much scientific attention<sup>4–9</sup> as the copolyester Vectra<sup>®</sup> A950, despite its outstanding mechanical properties.

## EXPERIMENTAL

### Materials and sample preparation

The liquid crystalline polymer (LCP) Vectra<sup>®</sup> B950 is a copolyesteramide containing 60% polyhydroxynaphthoic acid, 20% terephthalic acid and 20% aminophenol. The thermoplastic is a polyarylate (PAr Arilef U 1060, Solvey) of bisphenol A, with a 50:50 ratio of isophthalic acid/terephthalic acid. Before mixing, Vectra<sup>®</sup> B950 and PAr were dried at 100°C for 48 and 24 h, respectively.

The blends were prepared at 285°C using two different

mixing devices: a Kenics Static mixer (with five helicoidal elements) adapted to a capillary Sieglaff–McKelvey rheometer and a Brabender mixing head with two blades. Both basic polymers (Vectra<sup>®</sup> and PAr) were also extruded through the static mixer to subject all the materials to the same thermomechanical history.

### Rheological techniques

The materials were compressed at 285°C to obtain suitable samples (typically 1 × 2 × 15 mm) to be analysed in a Polymer Laboratories DMTA at frequencies ranging from 10<sup>-2</sup> to 10<sup>2</sup> Hz in bending mode. Storage modulus (*E'*) and loss factor ( $\tan \delta$ ) spectra were determined.

Viscosity measurements were carried out in an extrusion rheometer (Gottfert Rheograph 2002) with a length (*l*)/diameter (*d*) = 30 capillary and non-isothermal melt spinning was developed at 300°C using a spinning unit adapted to a Sieglaff–McKelvey rheometer with a *l/d* = 25.4 capillary. The draw ratio is defined as  $v_L/v_0$  where  $v_L$  is the winding speed and  $v_0$  is the speed at the exit of the capillary. The *E'* values of the fibres obtained at different draw ratios were determined in the DMTA (tensile mode).

## RESULTS AND DISCUSSION

### Incompatibility

Figure 1 shows the  $\tan \delta$  spectra of the original samples and the blends. The glass transition of PAr corresponds to the maximum in  $\tan \delta$  observed at 190°C, whereas the LCP presents a much smaller maximum at 137.5°C which corresponds<sup>10,11</sup> to the glass–nematic transition. This small value of the  $\tan \delta$  peak reflects the semicrystalline nature of the copolyesteramide. Figure 2 shows the glass transition temperature ( $T_g$ ) as a function of composition: in all the blends the two  $T_g$ s of the respective original polymers are present indicating incompatibility (phase separation) between the components. On the other hand, the values of  $\tan \delta$  peaks [ $(\tan \delta)_M$ ] show a linear dependence on composition (Figure 3) as could be

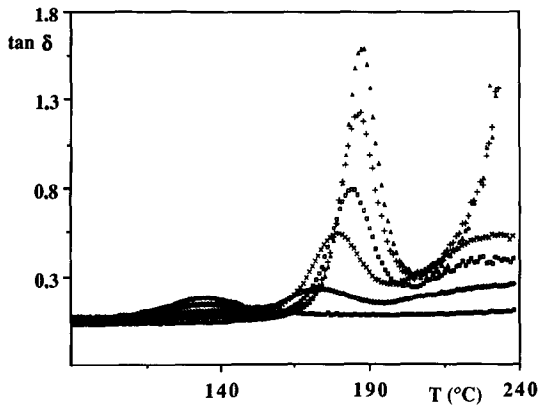


Figure 1 Loss factor as a function of temperature for various blends: (■) LCP; (◇) 80 LCP/20 PAr; (×) 60 LCP/40 PAr; (□) 40 LCP/60 PAr; (+) 20 LCP/80 PAr; (△) PAr

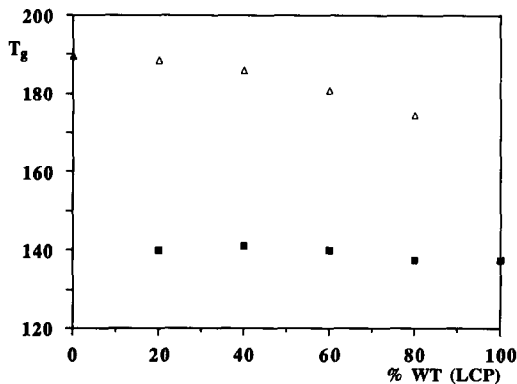


Figure 2 Glass transition temperatures corresponding to the PAr (△) and LCP (■) phases as a function of composition

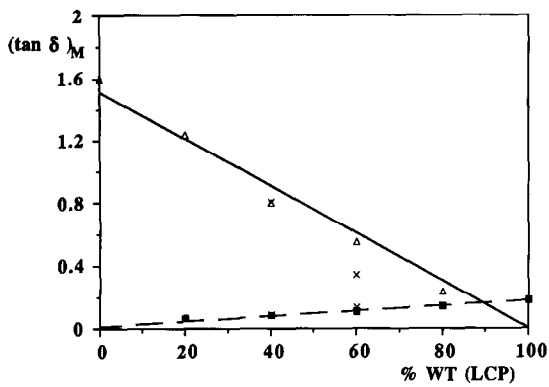


Figure 3 Values of the peaks of the loss factor for blends prepared in both mixing devices. Lines correspond to additivity rule: (△) PAr (Kenics); (■) LCP (Kenics) (×) Brabender (PAr and LCP)

expected for non-interacting polymers. Figure 3 shows the deviation from linearity observed for the 60 LCP/40 PAr blend prepared in the Brabender. This result reveals a difference between blends of the same composition but prepared in two different mixing devices.

*Differences between 60 LCP/40 PAr (Brabender) and 60 LCP/40 PAr (Kenics)*

The different viscoelastic behaviour observed in Figure 3 for blends of the same composition must be attributed to a different morphology. In order to have a general idea of the morphology of the 60 LCP/40 PAr blends

the samples obtained from both mixing devices were subjected to attack by chloroform which is a good solvent for PAr but does not attack Vectra® B950. We observed that blends prepared in the Brabender mixer were not attacked, whereas Kenics blends were partially dissolved. Figures 4a and b show photographs of extrudates (obtained in the rheometer) after 2 h in chloroform: the differences between the blends performed in the Brabender and in the Kenics Static mixer are remarkable. In the case of the 60 LCP/40 PAr (Brabender) blend the extrudate remains intact, while in the case of the blend prepared in the Kenics Static mixer the chloroform dissolves the PAr revealing the LCP fibres formed during the flow along the capillary. This result is due to the fact that in the first case Vectra® B950 constitutes the continuous phase, whereas in the Kenics blend PAr forms the matrix.

The viscoelastic behaviour of both blends is more extensively studied in Figures 5a and b where  $E'$  and  $\tan \delta$  are presented as functions of temperature. A block model<sup>12</sup> is applied (Appendix) to fit the experimental data using, respectively, LCP and PAr as the matrix. We observe that the results presented in Figures 4 and 5 are coincident: the blend attacked by chloroform (Figure 4b) presents viscoelastic data that can only be fitted using PAr as the matrix. In contrast, the blend that remains intact under the action of chloroform (Figure 4a) gives a viscoelastic behaviour that is explained by having LCP as the matrix. Further evidence of the different morphologies of 60 LCP/40 PAr blends is shown in Figure 6 where the viscosities of the original components and 60 LCP/40 PAr blends are presented as functions of shear rate. The data of both Brabender and Kenics blends have been fitted to the following equation<sup>13</sup>:

$$\eta_B = (1 - \lambda)\eta_M + \lambda \left[ \frac{\psi}{\eta_M} + \frac{(1 - \psi)}{\eta_D} \right]^{-1} \quad (1)$$

where the subscripts B, M and D refer to the blend, matrix and disperse phase, respectively, and  $\lambda\psi$  is equal

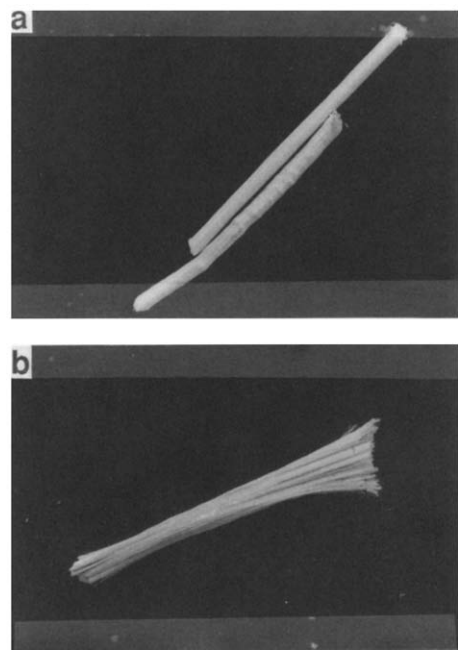
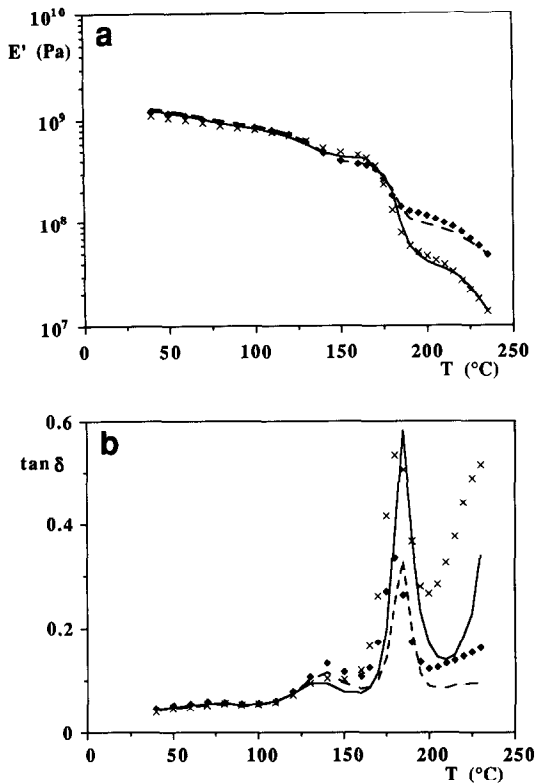
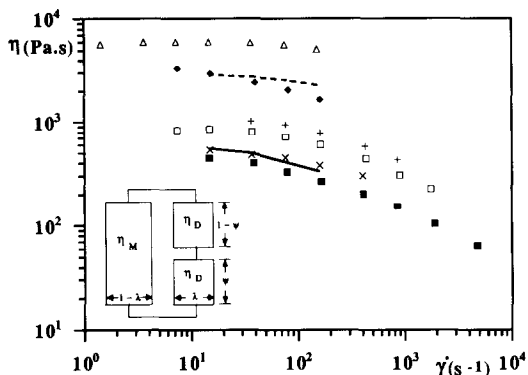


Figure 4 Extrudate of a 60 LCP/40 PAr blend prepared in (a) the Brabender device and (b) the Kenics mixer, after 2 h in chloroform



**Figure 5** (a) Storage modulus (bending mode) and (b) loss factor as a function of temperature for 60 LCP/40 PAR blends prepared in the Brabender device ( $\blacklozenge$ ) and the Kenics mixer ( $\times$ ). The lines correspond to a block-type model (Appendix): (—) matrix PAR; (---) matrix LCP



**Figure 6** Viscosity as a function of shear rate for various samples at 300°C: ( $\Delta$ ) PAR; ( $\blacklozenge$ ) 60 LCP/40 PAR (Brabender); (+) 20 LCP/80 PAR; ( $\square$ ) 40 LCP/60 PAR; ( $\times$ ) 60 LCP/40 PAR (Kenics); ( $\blacksquare$ ) LCP. The lines correspond to the model inset in the figure [equation (1)]

to the volume fraction of the continuous phase. When Vectra<sup>®</sup> B950 is used as the continuous phase, equation (1) agrees reasonably well with the Brabender blend data, whereas taking PAR as the continuous phase gives good agreement for the data of the blend prepared in the Kenics device. On the other hand, Figure 6 shows that Vectra<sup>®</sup> B950 can be used as a processing aid agent, since for low LCP content blends the viscosity visibly decreases.

#### Rheology and morphology

In the field of incompatible blends it has been established<sup>14</sup> that the low viscosity component encap-

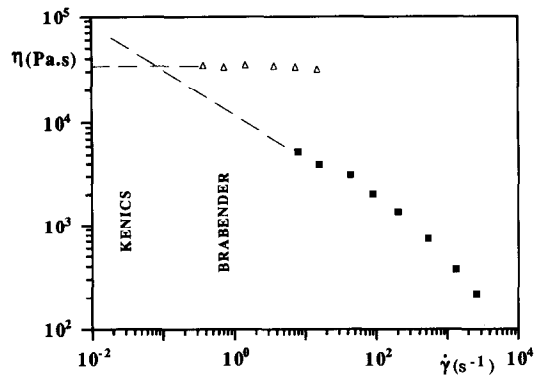


**Figure 7** Viscosity as a function of shear rate for pure polymers. Extrapolations are drawn assuming viscoplastic behaviour for Vectra<sup>®</sup> B950 and Newtonian behaviour for PAR: ( $\blacksquare$ ) LCP; ( $\triangle$ ) PAR

ulates the high viscosity component and becomes the continuous phase. It happens that, depending on the ratio of the mixing viscosities of the original polymers, the minor component can form the continuous phase. A certain kind of competition exists between the compositional and rheological parameters and this allows different morphologies to be obtained for the same blend composition. We think that the results we have obtained for 60 LCP/40 PAR blends must be discussed within this framework. Figure 7 gives viscosity as a function of shear rate for the components of the blends at the temperature at which mixing takes place. Mixing the polymers in the Kenics device gives rise to very low shear rates, since the velocity of the piston is  $0.01 \text{ cm s}^{-1}$  and the diameter of the barrel where the helices are adapted is 8 mm. However the shear rates developed in the Brabender mixing head are considerably higher. Figure 7 shows the shear rates corresponding to the Kenics and Brabender devices. At this low temperature the viscoplastic behaviour of the LCP can be foreseen<sup>15</sup>, so we can deduce that at low shear rates (Kenics mixing operation) PAR is less viscous than Vectra<sup>®</sup> B950 and becomes the continuous phase. This is confirmed by the fact that the load force necessary to extrudate PAR through the Kenics Static mixer is lower than that of Vectra<sup>®</sup> B950. In contrast, mixing in the Brabender gives blends with LCP as the continuous phase, as a consequence of the lower viscosity of this component at high shear rates.

#### Effect of draw ratio on storage modulus

For LCPs it has been observed<sup>16–20</sup> that the development of orientation during the melt spinning leads to an increasing Young's modulus as a function of draw ratio until a limiting plateau is reached. An explanation for the variation of modulus with draw ratio has been envisaged by Alderman and Mackley<sup>16</sup> in terms of the velocity profile rearrangement at the exit of the die. Figure 8 shows  $E'$  at 30°C as a function of draw ratio: it is worth pointing out the sensitivity to draw ratio shown by the LCP, whereas the modulus of PAR remains constant. On the other hand, we also note that the morphological and rheological differences between the 60 LCP/40 PAR blends prepared, respectively, by the Kenics Static mixer and the Brabender mixing head, are not reflected in the modulus at 30°C.

The effect of draw ratio for different compositions is seen in Figure 9 where  $E'$  is plotted against composition

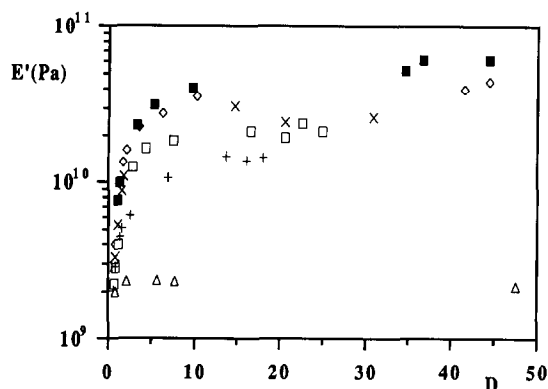


Figure 8 Storage modulus at 30°C as a function of draw ratio: (■) LCP; (◇) 80 LCP/20 PAR; (×) 60 LCP/40 PAR (Kenics and Brabender); (□) 40 LCP/60 PAR; (+) 20 LCP/80 PAR; (△) PAR

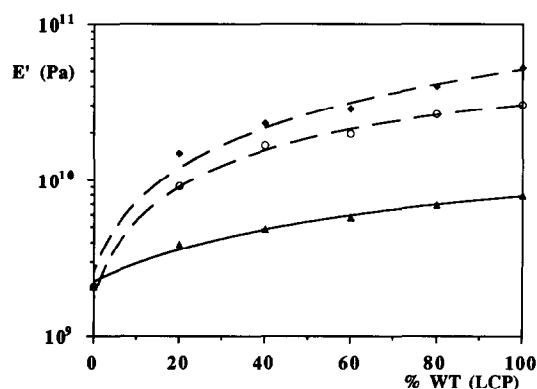


Figure 9 Storage modulus at 30°C and various draw ratios as a function of composition. Draw ratio: (▲) 1; (○) 5; (◆) 20

for three draw ratios (1, 5 and 20). The reinforcing action of Vectra® B950 is obvious: relatively small quantities of LCP in the blend (e.g. 20%) give rise to a 700% increase in the modulus of fibres prepared at high draw ratios.

## CONCLUSIONS

Dynamical mechanical analysis reveals two  $T_g$ s in all the blends prepared in the Brabender mixing head and in the Kenics Static mixer. Both glass transitions correspond, respectively, to the LCP phase and the PAR phase: the polymers are, therefore, incompatible and in mixing give rise to heterogeneous blends.

The differences between the 60 LCP/40 PAR blend prepared in the Brabender and in the Kenics are obvious. The following features can be pointed out:

1. Chloroform attacks the Kenics prepared blend (dissolving it partially) but does not attack the blend mixed in the Brabender device.
2. Different  $E'$  and  $\tan \delta$  spectra are obtained for both blends although the composition is the same. A Takayanagi-type model fits the experimental values well using PAR as the continuous phase for Kenics blends and Vectra® B950 for Brabender blends.
3. The viscosity is higher for the 60/40 blend prepared in the Brabender than for that, of the same composition,

prepared in the Kenics Static mixer. The shear rates involved in each mixing process are different, giving viscosity ratios  $>1$  for the Kenics and  $<1$  for the Brabender. This produces a change in morphology which accounts for the above-mentioned chemical and viscoelastic differences.

Fibres obtained from non-isothermal melt spinning give increasing  $E'$  as a function of draw ratio. The effect is more remarkable for LCP-rich blends, but is also noticeable for 20 LCP/80 PAR blends: a 700% increase in modulus with respect to PAR can be attained spinning at high draw ratios.

## REFERENCES

- 1 Calundann, G. W. and Jaffe, M. Proceedings of The Robert A. Welch Conferences on Chemical Research XXVI Synthetic Polymers, Houston, Texas, 1982
- 2 Dutta, D., Fruitwala, H., Kohli, A. and Weiss, R. A. *Polym. Eng. Sci.* 1990, **30**, 1005
- 3 Brostow, W. *Polymer* 1990, **31**, 979
- 4 Chung, T. S. and McMahon, P. E. *J. Appl. Polym. Sci.* 1986, **31**, 965
- 5 La Mantia, F. P. and Valenza, A. *Polym. Eng. Sci.* 1989, **29**, 625
- 6 Paci, M., Liu, M., Magagnini, P. L., La Mantia, F. P. and Valenza, A. *Thermochim. Acta* 1988, **137**, 105
- 7 La Mantia, F. P., Valenza, A., Paci, M. and Magagnini, P. L. *J. Appl. Polym. Sci.* 1989, **38**, 583
- 8 La Mantia, F. P., Saiw, M., Valenza, A., Paci, M. and Magagnini, P. L. *Eur. Polym. J.* 1990, **26**, 323
- 9 La Mantia, F. P., Valenza, A., Paci, M. and Magagnini, P. L. *Polym. Eng. Sci.* 1990, **30**, 7
- 10 Gonzalez, J. M., Muñoz, M. E., Cortazar, M., Peña, J. J. and Santamaria, A. *J. Polym. Sci., Polym. Phys. Edn.* 1990, **28**, 1533
- 11 Green, D. I., Davies, G. R., Ward, I. M., Alhaj Mohammed, M. H. and Abdul Jawad, S. *Polym. Adv. Technol.* 1990, **1**, 41
- 12 Gomez Ribelles, J. L., Maño Sebastia, R., Marti Soler, R., Mauleon Pradas, M., Ribes Creus, A. and Suay Anton, J. J. *J. Appl. Polym. Sci.* 1991, **42**, 1647
- 13 Suto, S. *J. Appl. Polym. Sci.* 1987, **34**, 1777
- 14 Avgeropoulos, G. N., Weissert, F. C., Biddison, P. H. and Böhn, G. G. A. *Rubber Chem. Technol.* 1976, **49**, 93
- 15 Wissbrun, K. F. *J. Rheol.* 1981, **25**, 619
- 16 Alderman, N. I. and Mackley, M. R. *Faraday Discuss.* 1985, **79**, 149
- 17 Cuculo, J. A. and Chen, G.-Y. *J. Polym. Sci., Polym. Phys. Edn.* 1988, **26**, 179
- 18 Yang, D.-K. and Krigbaum, W. R. *J. Polym. Sci., Polym. Phys. Edn.* 1989, **27**, 1837
- 19 Nobile, M. R., Acierno, D., Incarnato, L., Amendola, E., Nicolais, L. and Carfagna, C. *J. Appl. Polym. Sci.* 1990, **41**, 2723
- 20 Blizard, K. G., Federici, C., Federico, O. and Chapoy, L. L. *Polym. Eng. Sci.* 1990, **30**, 1442

## APPENDIX

The block model applied is<sup>1,2</sup>:

$$E'_B = \frac{AB + CD}{B^2 + C^2} \quad (A1)$$

$$\tan \delta_B = \frac{CB - AD}{AB + CD} \quad (A2)$$

where

$$A = (M'E'_M - M''E''_M)$$

$$B = (\xi M' + \bar{\xi} E'_M)$$

$$C = (M''E'_M + M'E''_M)$$

$$D = (\xi M'' + \bar{\xi} E''_M)$$

and

$$M' = \psi KE'_D + \bar{\psi} E'_M \quad M'' = \psi KE''_D + \bar{\psi} E''_M$$

$$\psi = \frac{\phi}{1 - \xi} \quad \xi = \lambda(1 - \phi)$$

$$\bar{\xi} = 1 - \xi \quad \bar{\psi} = 1 - \psi$$

where B, M and D refer, respectively, to the blend, matrix and dispersed phase and  $\phi$  is the volume fraction of the dispersed phase,  $\lambda$  is the volume fraction of the matrix in series, [i.e.  $\lambda(1 - \phi) = \xi$  is the total volume fraction in series].

The efficiency coefficient  $k$  summarizes the misalignment of the fibres in the blend, the lack of perfect adhesion

between matrix and reinforcement and other possible causes of reduced reinforcement efficiency.

The values of  $\lambda$  and  $K$  which show better agreement between experimental and model behaviour are summarized in Table A1.

**Table A1** Values of the constants in equations (A1) and (A2) to fit the experimental data in different temperature ranges

$\lambda$	Brabender		Kenics		
	$K$	$\Delta T$	$\lambda$	$K$	$\Delta T$
0.835	0.63	40–140	0.1	0.62	40–165
	0.52	140–165		0.25	165–235
	0.30	165–235			